Experimental Study of the Ion Critical Gradient Length and Stiffness Level and the Impact of Rotational Shear in the JET tokamak

P.Mantica 1), D.Strintzi 2), T.Tala 3), C.Giroud 4), T.Johnson 5), H.Leggate 4), E.Lerche 6), T.Loarer 7), A.G.Peeters 8), A. Salmi 3), S.Sharapov 4), D.Van Eester 6), P.C. de Vries 4), L.Zabeo 4), K.-D.Zastrow 4) and JET-EFDA contributors[#]

JET-EFDA, Culham Science Centre, OX14 3DB, Abingdon, UK
1) Istituto di Fisica del Plasma CNR-EURATOM, via Cozzi 53, 20125 Milano, Italy
2) National Technical University of Athens, Association Euratom - Hellenic Republic, GR-15773 Athens, Greece
3) Association EURATOM-Tekes, VTT, P.O. Box 1000, FIN-02044 VTT, Finland
4) Culham Science Centre, EURATOM/UKAEA Fusion Association, Oxon. OX14 3DB, UK
5) Association EURATOM - VR, Fusion Plasma Physics, EES, KTH, Stockholm, Sweden
6) LPP-ERM/KMS, Association Euratom-Belgian State, TEC, B-1000 Brussels, Belgium
7) CEA Cadarache, Association EURATOM-CEA, 13108, St Paul-Lez-Durance, France
8) Centre for Fusion Space and Astrophysics, University of Warwick, Coventry 7AL, UK

 # see Annex 1 in ROMANELLI, F., et al., "Overview of JET results", Fusion Energy 2008 (Proc. 22nd Int. Conf. Geneva, 2008), OV/1-2, IAEA, Vienna

e-mail contact of main author: mantica@ifp.cnr.it

Abstract. Experiments have been carried out in the JET tokamak in order to determine the critical ion temperature inverse gradient length ($R/L_{Ti} = R|\nabla T_i|/T_i$) for the onset of Ion Temperature Gradient modes and the stiffness of T_i profiles with respect to deviations from the critical value. The existence of a threshold in R/L_{Ti} has been assessed and its value found in close agreement with linear GS2 gyro-kinetic calculations. The ion stiffness level is high and keeps R/L_{Ti} close to the linear threshold irrespective of the amount of core ion heating. This finding is not in agreement with non-linear GS2 calculations, yielding significantly higher R/L_{Ti} values than the linear threshold. Comparison of plasmas with different values of toroidal rotation indicates a significant increase in R/L_{Ti} in rotating plasmas. Various observations allow to conclude that such increase is mainly due to a decrease of the stiffness level with increasing rotation, rather than to a mere up-shift of the threshold, as commonly predicted by theory. This finding has implications on the interpretation of present day experimental results on the effect of rotation on confinement as well as on extrapolations to future machines.

1. Introduction

The anomalous character of ion heat transport in tokamaks, one order of magnitude higher than the level foreseen for collisional transport, is a long dated experimental observation. Recent studies are reported e.g. in [1-3]. A comprehensive theoretical description of turbulent ion heat transport as driven by Ion Temperature Gradients (ITG) modes has been developed and applied to physics based predictions of confinement in present and future devices [4-7]. ITGs are excited above a critical value for the ion temperature inverse gradient length ($R/L_{Ti}=R|\nabla T_i|/T_i$, with R the major radius of the torus) and drive an increase in ion transport which tends to prevent the T_i profiles from departing from the threshold value. This property leads to stiffness of temperature profiles with respect to changes in heating profiles. The level of stiffness characterizes how strongly the temperature profiles are tied to threshold. Experimental observations in several devices of the correlation between edge and core T_i values [1,8-10] support this theoretical picture. However, no dedicated experimental studies have yet been performed demonstrating the existence and value of an ion critical gradient length, its parametric dependences on plasma parameters and up-shifts due to rotational shear or non-linear effects, as predicted by theory. Also, no experimental determination of the response of the ion heat flux (q_i) to an increase in R/L_{Ti}, which indicates the stiffness level, has yet been made, although recent T_i modulation experiments in JET [11] have provided the first measurements of the ion stiffness level by determining the local slope of the q_i vs R/L_{Ti} curve.

The issue is of high relevance for the operation of future generation tokamak devices, such as

ITER or DEMO. Simulations in ITER geometry indicate that an increase of R/L_{Ti} by 1 unit, from 4 to 5, at fixed pedestal, leads to an increase by ~50% of central T_i, by ~20% in the confinement enhancement factor H98, and to a doubling of the α-power and fusion gain Q. Therefore it is important to investigate what value of R/L_{Ti} is achievable is ITER, which for a given power level and pedestal height depends on threshold and stiffness. Theoretical predictions of these quantities must be validated against experiment to allow confidence in the extrapolation. In this paper first experiments on JET aiming at the identification of the ITG threshold and stiffness in plasmas with low rotation, comparison with theory, and an experimental evaluation of the impact of rotation will be presented.

2. Experimental results in steady-state approach

The JET tokamak (R=2.96m, a=1 m) is equipped with a high quality active Charge Exchange Spectroscopy (CX) diagnostics for T_i and toroidal rotation (ω_t) measurements and a multi-frequency Ion Cyclotron Resonance Heating (ICRH) system for flexible and fairly localized ion heating either using (H)-D or (^{3}He)-D minority schemes. These tools, together with JET's large size and low normalized ion gyro-radius, make it an ideal device where to perform on ions studies of threshold and stiffness level as prior performed on electrons [12-14]. Experimentally the identification of the ITG threshold and stiffness level requires a scan of the core q_i at constant edge flux, to keep edge properties constant, whilst maintaining reasonably unchanged other plasma parameters such as density, safety factor profile, T_e/T_i, Z_{eff}, rotation. Both electron and ion heat fluxes are predicted by theory to follow a gyro-Bohm scaling, at least for low values of the normalized gyro-radius, so that q_i can be written as [15]

$$q_i = q_i^{res} + n_i \ q^{1.5} \ \chi_s \frac{T_i^2 \rho_i}{eBR^2} \ \frac{R}{L_{T_i}} f\left[\frac{R}{L_{T_i}} - \frac{R}{L_{T_{i\,crit}}}\right] \cdot H\left[\frac{R}{L_{T\,i}} - \frac{R}{L_{T_{i\,crit}}}\right] \quad (1)$$

where q_i^{res} is the residual flux, incorporating the neoclassical flux and possible contributions to ion transport not driven by ITG, n_i the density, q the safety factor, B the magnetic field, e the electron charge, ρ_i= $(m_i\ T_i)^{1/2}/eB$, m_i the ion mass and H the Heaviside step function. Therefore, from the curve of the gyro-Bohm normalized q_i^{norm} vs R/L_{Ti}, the threshold R/L_{Ticrit} can be identified as the intercept at neoclassical flux and the stiffness level χ_s can be inferred from the slope. This implies a normalization of the heat flux over a factor $n_i\ q^{1.5}\ T_i^{5/2}/R^2B^2$. Because the experiments considered in this paper have similar values of Z_{eff} ~ 2-2.5, for simplification of the analysis n_e has been used instead of n_i for the normalization of the ion heat flux. The normalization is not important for the identification of the threshold but is essential to extract from the experimental data the correct intrinsic stiffness level χ_s. Far from threshold q_i is theoretically foreseen to be linear with R/L_{Ti} [16]. In the range of q_i covered by the experiments, not too far from threshold, the experimental uncertainties do not allow to distinguish between linear and quadratic dependence. To allow comparison with previous work on electron stiffness, following the assumptions of the semi-empirical critical gradient model (CGM) described in [17], in the empirical modelling described below $f(R/L_{Ti})$ was assumed to be linear, so that q_i is quadratic in R/L_{Ti}.

The experiment was performed in JET L-mode plasmas with B_T=3.36T, I_p=1.8MA, q_{95}~6 (to minimize core sawtooth activity), n_{e0}~3-4 10^{19}m^{-3}, $\nu^*_{(\rho=0.33)}$~0.2, 0.9<T_e/T_i~1.2. Typical plasma profiles are shown in Fig.1 as a function of the normalized toroidal minor radius (ρ_{tor}=ρ_t/ρ_t^{edge} where ρ_t =$\sqrt{\Phi/\pi B_0}$, with Φ the toroidal magnetic flux, and ρ_t^{edge} is the value of ρ_t at the plasma boundary. The need to reach low values of q_i^{norm} to identify the threshold requires to minimize the central power from Neutral Beam Injection (NBI). Therefore the experiment was done in low rotating plasmas, retaining only the diagnostic NBI beam for CX. Most of heating was then provided by ICRH, using the multi-frequency capability to vary the ion power distribution between on- and off-axis.
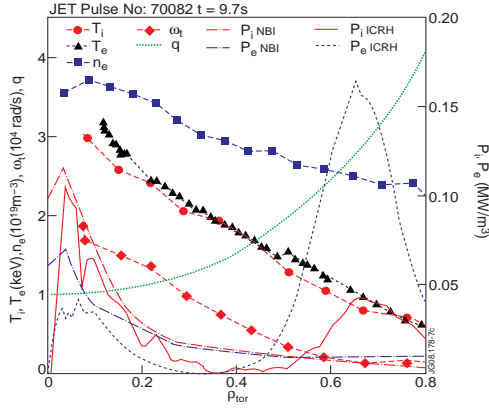
FIG.1 Profiles of T_i, T_e, n_e, ω_t, q, ICRH and NBI power deposition for shot 70082, t=9.7 s, within the ITG study series. ICRH power in H-(D) scheme was parted between on- and off-axis, corresponding to a point about mid-way in the q_i^{norm} excursion in FIG.2.

ICRH power was 3-6 MW and NBI power 1.5 MW for the CX diagnostic. ICRH was applied in (H)-D scheme with H concentration ~8%, with 30-60% of the ICRH core power delivered to ions, and in (^{3}He)-D scheme with ^{3}He concentration ~7%, with 50-80% of the ICRH core power delivered to ions. Frequencies of 51 MHz and 42 MHz were used for on- and off-axis deposition respectively in (H)-D and 33 MHz and 29 MHz in (^{3}He)-D. Power was shifted from off-axis to on-axis either from shot to shot, or having 2-3 steps within a single shot. Values of R/L_{Ti} were averaged in time over the stationary intervals and calculated with respect to the flux surface minor radius defined as $\rho=(R_{out}-R_{in})/2$, where R_{out} and R_{in} are the outer and inner boundaries of a given flux surface on the magnetic axis plane. This choice allows direct comparison with R/L_{Ti} values predicted by gyro-kinetic simulations. The values of q_i have been calculated using the SELFO [18] code for ICRH and the PENCIL [19] code for the NBI power. Profiles of ICRH and NBI ion and electron power are shown in Fig.1. The PION code [20], most commonly used at JET for ICRH deposition, was in fact found to predict faulty power profiles in the plasma conditions of the experiment. The resulting q_i^{norm} vs R/L_{Ti} plot is shown in Fig.2 (red full circles).
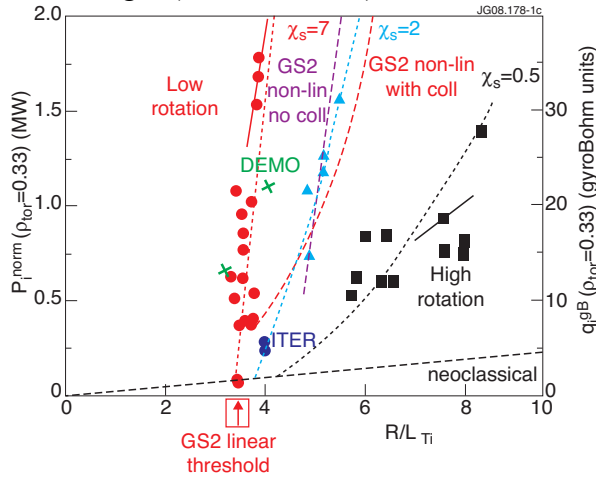

FIG.2. Normalized ion heat flux at $\rho_{tor}=0.33$ vs R/L_{Ti} for similar plasmas with different levels of rotation. Dots represent experimental data and lines simulations. ● : $1<\omega_{t0}<2$ $10^4 rad/s$, ▲ : $3<\omega_{t0}<4$ $10^4 rad/s$, ■ : $5<\omega_{t0}<6$ 10^4 rad/s. The dashed black line is indicative of the neoclassical transport. The 2 segments indicate the local slope deduced from modulation. The 3 dotted lines are simulations using the CGM with different values of χ_s. The dashed thicker red and violet lines are non-linear GS2 simulations with and without collisions, and the red arrow indicates the GS2 linear threshold for the low rotation shots.

The points at neoclassical level were obtained by slowly modulating the NBI CX beam to measure just after switch-on the T_i profile corresponding to zero NBI power. Statistical error bars are not plotted for clarity's sake, they are typically $\Delta R/L_{Ti} \sim \pm 0.3$-$0.6$ and $\Delta q_i^{norm} \sim \pm 0.1$ MW. The gyro-Bohm normalization has been applied to q_i in two ways, to meet the inclinations of both experimentalists and theoreticians. The left scale of Fig.2 indicates the total power in MW within $\rho_{tor}=0.33$ and is normalized over $n_e T_i^{5/2}/R^2 B^2$ by rescaling the power to reference local values $T_i=1.85$ keV, $n_e=3\ 10^{19}$ m^{-3}, $B_T=3.36T$. The $q^{1.5}$ dependence was not included in the normalization because q has small variations across the dataset (q~1.2-1.5) and with large relative experimental uncertainties. The right scale indicates the values of q_i at $\rho_{tor}=0.33$ in gyro-Bohm units, i.e. q_i^{gB} [gB-units]= q_i [MW/m^2] / $[(\rho_i/R)^2 v_{ith} n_i T_i]$, where $v_{ith} = \sqrt{T_i/m_i}$. The threshold is well identified experimentally in Fig.2 as the intercept at neoclassi-

cal heat flux. The ion stiffness level appears to be high, as the available excursion of q_i^{norm} by over one order of magnitude does not lead to a significant change in R/L_{Ti} The ITER and DEMO positions marked in Fig.2 are from simulations using the GLF23 [21] transport model with two assumptions for the pedestal. They will be discussed in Sect.5.

Comparison with highly rotating JET plasmas at high NBI power with similar main parameters, although with obviously higher q_i and T_i, but still same $T_e/T_i \sim 1$ and similar range of q_i^{norm}, indicates a significant increase of R/L_{Ti} with increasing rotation (blue triangles and black squares in Fig.2). Central rotation and rotation gradient vary by up to a factor 6. Other parameters have minor variations, with the exception of the ratio $R/L_{Te}/R/L_{Ti}$, which is ~ 1 in high rotation shots, and varies between 1.2 and 1.9 with increasing heat flux in low rotation shots. This is inherent in the fact that electrons are found less stiff than ions at low rotation, and the unavoidable fraction of ICRH electron power is sufficient to induce an increase of R/L_{Te} whilst R/L_{Ti} is blocked at the threshold by the high ion stiffness. On the other hand, since the ion heat flux driven by R/L_{Te} is generally negligibile [11], we do not believe that such variation may affect our conclusions. The shearing rate ω_{ExB} at $\rho_{tor}=0.33$ is calculated using the transport code JETTO [22] assuming neoclassical poloidal velocity and is found to vary from $1.1 \ 10^4 s^{-1}$ to $2.2 \ 10^4 s^{-1}$ for two typical shots of the low and high rotation sets.

Since in the high rotation discharges in Fig.2 the threshold is not directly identified due to the large values of q_i^{norm}, the key question is to determine if such increase in R/L_{Ti} is due to an effect of rotational shear on the threshold only, in accordance with theory predictions (i.e. keeping the same slope for all curves), or also on the stiffness level. In the first case, one would need a shift in threshold $\Delta R/L_{Ti} \sim 4$, which is much larger than the value $\Delta R/L_{Ti} \sim 1$ predicted by the so-called "Waltz rule" [23]: $\gamma = \gamma_{lin} - \alpha_E \ \omega_{ExB}$ with $\alpha_E \sim 0.6$ [24]. Such a high shift in threshold is very difficult to justify especially given the high stiffness measured in the low rotation shots. Assuming instead the validity of the Waltz rule for the shift in threshold, as in Fig.2, an upper limit for the change in the intrinsic stiffness coefficient χ_s has been estimated by fitting the data using the CGM [17]. The dotted lines in Fig.2 indicate a change of χ_s from 7 to 0.5 with increasing rotation, leading to a factor 3 increase in R/L_{Ti} at similar values of the normalized heat flux. This implies that the variation of stiffness has a much larger impact on R/L_{Ti} than the variation of threshold. Since this is a new effect, apparently not predicted by present theories, additional experimental evidence has been sought to confirm such finding.

3. Experimental results in perturbative approach

First of all, T_i modulation experiments using (^3He)-D scheme provide a direct measurement of the local slope in the q^{norm} vs R/L_{Ti} diagram. First experiments in highly rotating plasmas [11], indicating moderate stiffness levels, have been now repeated both in low and high rotation plasmas to seek an independent confirmation of the factor 10 variation of stiffness level observed in the steady-steady plot in Fig.2. 35 power modulation cycles at 6.25 Hz were performed, with about 3 MW of modulated ICRH power with on-axis deposition and duty-cycle 70%, to provide both 1st and 2nd harmonic components of the modulation. Fig.3 shows the amplitude (A) and phase (φ) profiles of the T_i perturbation at 6.25 and 12.5 Hz for two shots belonging respectively to the red circle and black square sets in Fig.2. It is immediately evident from the slopes of A and φ in Fig.3 that the incremental diffusivity $\chi_i^{inc} = -\partial q_i/n_i \partial \nabla T_i$ is much higher in the low rotation shot. A simple analysis calculating χ_i^{inc} from of the φ slopes ($\chi_i^{inc} = 3/4\omega/\varphi'^2$, [9]) yields $\chi_i^{inc} = 12 \ m^2/s$ at low rotation and $2.6 \ m^2/s$ at high rotation. The ratio with the power balance heat diffusivity ($\chi_i^{PB} = -q_i/n_i \nabla T_i$) is 5 and 1.9 respectively. Normalizing by $T_i^{3/2}$ further enhances the difference in χ_i^{inc}, because high rotation shots are also hotter. The slopes derived from this analysis are indicated in Fig.2 by the two solid segments. A more refined determination of the intrinsic stiffness coefficient χ_s was obtained with a time

dependent transport simulation with the ASTRA code [25] using the CGM model [17]. The resulting A and φ profiles are also plotted in Fig.3. The width of the ion deposition and the ion coupled power have been taken from SELFO calculations, as well as the indication of the fast ion slowing down that determines the φ absolute values. The electron temperature is modelled as well, because a significant T_e modulation is also measured, but the simulations show that the contribution to the T_i modulation due to collisional coupling is about 10% at 6.25 Hz and insignificant at 12.5 Hz. The modulation data (and the steady-state, not shown) can overall be satisfactorily fitted using $R/L_{Ti,crit}$=3.5, χ_s=3 at low rotation and $R/L_{Ti,crit}$=4, χ_s=0.3 at high rotation. We conclude that the T_i modulation data directly confirm the factor 10 decrease in stiffness level seen in Fig.2 with increasing rotation. The small discrepancy in χ_s values with respect to those indicated in Fig.2 may depend on the fact that the modulation extracts χ_s from a single shot but fitting the spatial profiles of A and φ with an effective stiffness scaling with radius as in Eq.(1), whilst the steady-state analysis of Fig.1 is local at ρ_{tor}= 0.33, but the fit is then made on a set of shots. In addition, one must be aware that the uppermost points in the low rotation shots in Fig.2 have T_e/T_i=1.1-1.2, which implies a downshift in threshold from 3.6 to 3.2, yielding some overestimate of the stiffness coefficient.
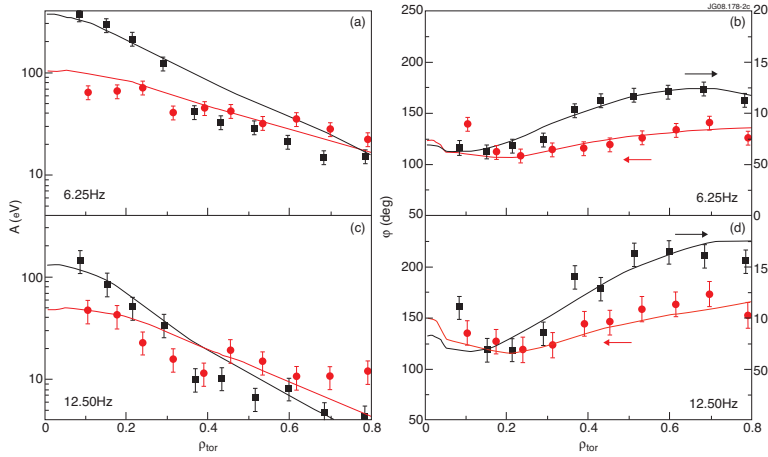

FIG.3 Experimental (dots) and simulated with CGM (lines) profiles of A and φ at 6.25 and 12.5 Hz, for a low rotation (73221, red circles) and a high rotation shot (73224, black squares).

4. Additional supportive results

Various evidence supportive of the previous results has been added to the results of the two main dedicated experiments illustrated in Sect.2 and 3. An exploration of the normalized q_i vs R/L_{Ti} dependence by varying n_i and T_i at fixed q_i, such as in L-H or type III to type I transitions also indicates moderate ion stiffness in high rotation plasmas. This is shown in Fig.4. On the other hand, experiments in which NBI power is substituted with ICRH (H)-D power at constant total power have also been performed in JET H-mode plasmas [26] and the resulting q_i^{norm} vs R/L_{Ti} plot is shown in Fig.5. Although these experiments do not allow keeping the same T_e/T_i for low and high rotation, due to the larger fraction of electron heating in ICRH (H)-D scheme, they confirm the high level of stiffness in low rotation plasmas. Unlike in the cases of Fig.2, due to the constraint of preserving the total power in this series of discharges, high rotation NBI dominant plasmas did not achieve as high range of variation of q_i^{norm} as low rotation ICRH dominant plasmas due to the broader power deposition of NBI compared with ICRH. Therefore whilst the small shift in threshold due to the combined effect of increased rotational shear and lower T_e/T_i is visible, nothing can be assessed on the decrease of the stiffness level in the high rotation case. For this reason, the conclusion that rotation does not affect core confinement as drawn from this type of experiments e.g. in [27] is unjustified.

Finally, the comparison of co- and counter-NBI plasmas with otherwise identical parameters (by reversing B_T and I_p in a dedicated campaign) shows that counter-NBI plasmas with flat rotation profiles exhibit much lower R/L_{Ti} than co-NBI plasmas with peaked rotation. The

comparison of ω_t and T_i profiles for a representative pair of co- and counter-NBI discharges is shown in Fig.6. The flatter and lower toroidal rotation in the counter-NBI case is ascribed to off-axis torque deposition, also shown in Fig.6a [28]. The non-normalized q_i is similar as shown in Fig.6b (only 25% smaller q_i in the counter-NBI case, which does not in itself justify the dramatic T_i decrease). Due to the low T_i, the counter-NBI shot has a higher normalized heat flux, nevertheless a dramatic reduction of R/L_{T_i} from 5.2 to 3.5 is observed (Fig.6b).
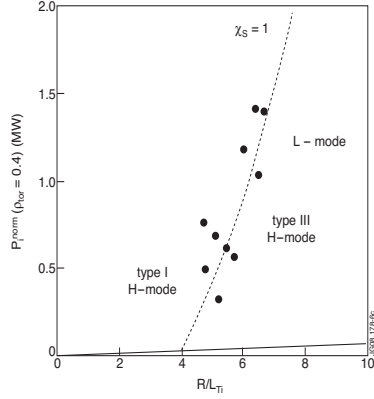
FIG.4: P_i^{norm} at $\rho_{tor}=0.4$ vs R/L_{T_i} for similar high rotation plasmas (66423 -32-33-34) in which the excursion in the Y axis is via changes of edge T_i at fixed q_i. The line is the CGM model.
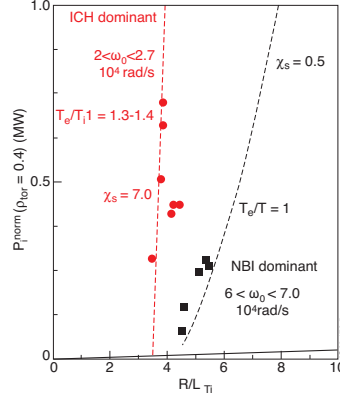
Fig.5: P_i^{norm} at $\rho_{tor}=0.4$ vs R/L_{T_i} in a set of H-mode shots (50623-50630; 52092 -52100) where dominant NBI power (black squares) was substituted with dominant ICRH power (red circles). The lines are the CGM model.
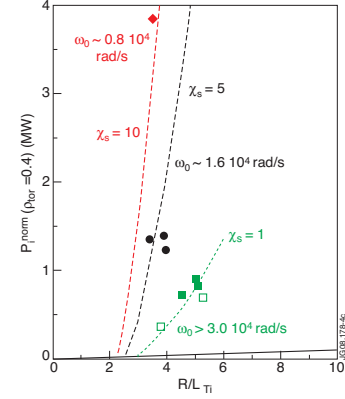
FIG.7 . P_i^{norm} at $\rho_{tor}=0.4$ vs R/L_{T_i} for co- (open symbols-58418) and counter-NBI (full symbols - 59630, 59637) discharges. Different rotations are marked with different symbols/colors. The lines are the CGM model.
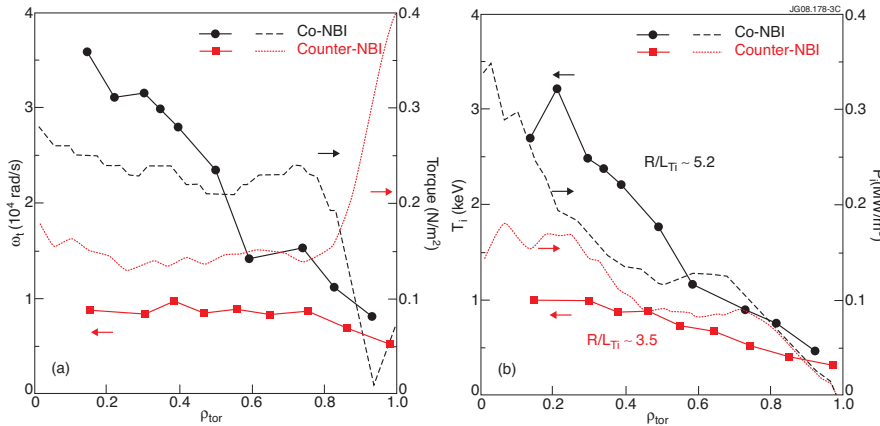

FIG.6. Comparison of (a) toroidal rotation and torque and (b) T_i and ICRH_NBI ion power profiles for a pair of similar JET discharges with co- (black circles and dashed lines) and counter-NBI (red squares and dotted lines).

In a q_i^{norm} vs R/L_{T_i} type of plot, the analysis of these pairs of co- and counter-NBI shots yields Fig.7, which makes use of various times during the density ramp-up leading to rotation decreasing in the counter-NBI case, and remaining peaked in the co-NBI case. The final states of co- and counter NBI shots (as shown in Fig.6) indicate again a very important difference in stiffness level, whilst being compatible with a similar threshold. Lines in Fig.7 are indicative of the CGM model stiffness levels compatible with the data.

Overall, we conclude that the available experimental evidence can be interpreted in a consistent framework only assuming a significant effect of rotation on ion stiffness level in addition to a smaller one on threshold.

5. Gyro-kinetic simulations

The GS2 gyro-kinetic code [29] has been used linearly and non-linearly to compare theory predictions with the results of the ITG threshold study in low rotation plasmas. The code does not include background ExB shear and thus cannot address effects of sheared plasma rotation.

Good agreement is found between the linear GS2 threshold (indicated by the arrow in Fig.2) and the value found in the experiment. The GS2 linear threshold has also been cross-checked with the linear threshold by the GENE [30], GKW [31] and GYRO [32] gyro-kinetic codes with very close match amongst the different codes. Minor variations were found in the linear threshold across the discharges in Fig.2, indicating that the increase in R/L_{Ti} at high rotation cannot be ascribed to a change in linear threshold associated to minor variations of plasma parameters. Parameter scans indicate that in these plasmas the linear threshold is mainly sensitive to T_e/T_i and q, whilst R/L_n and magnetic shear play a minor role. The non-linear GS2 predictions are drawn in Fig.2 as a short-dashed red and long-dashed violet lines, with and without ion-electron collisions respectively. Adding also ion-ion collisions does not change the curve. The collisionless runs yield a slope close to the experimental one, but an up-shifted non-linear threshold $R/L_{Ti} \sim 4.8$, with a significant Dimits shift. The experimental data however do not support such shift and remain close to the linear threshold. The collisional runs, which have to be regarded as more realistic, have a similar slope far from threshold, whilst approaching the threshold they deviate from the linear trend indicating a finite transport below the up-shifted threshold. In this case the non-linear threshold coincides with the linear one and the curve yields no prediction of a non-linear up-shift. However, the stiffness level in the q_i^{norm} range of the experiments turns out then to be significantly lower than in experiment. We conclude that non-linear GS2 simulations are not found in agreement with experiments. The new result of a significant decrease in stiffness level when increasing rotation cannot be addressed by GS2 and requires more complex numerical tools. To our knowledge, no prediction in this direction exists so far and deeper theoretical investigation is required.

5. Discussion and Conclusions

The implication of these findings is that rotation effects on stiffness cannot be ignored in addition to effects on threshold when interpreting experiments in present machines aimed at identifying the role of rotation on confinement, such as comparison of balanced vs unbalanced NBI [33,34], effects of varying B_T ripple [35], influence of resonant magnetic field perturbations [36]. Such results require careful assessment before being used for extrapolations to future devices. Depending on how close to threshold ITER or DEMO will operate, the smaller effect of rotation on threshold may or may not dominate over the effect on stiffness. In Fig.2 the ITER and DEMO positions are marked based on GLF23 simulations, with two different choices for the pedestal height. ITER is found to lie near threshold due to the low normalized heat flux, therefore ITER R/L_{Ti} will not benefit from the presently found effect of rotation on stiffness, but will rather be determined by the rather small threshold up-shift due to rotation. Based on the results of this paper, it is not clear that it will benefit from a more significant non-linear up-shift. DEMO on the other hand is expected to operate with a higher normalized heat flux, and would benefit of both threshold and stiffness improvements with rotation. In any case, blind extrapolations of the size of the effect of rotation on core confinement from present device experiments without knowing in which point of the diagram q_i^{norm} vs R/L_{Ti} the experiment is carried out and in which point ITER/DEMO will operate are not legitimate.

In summary, experimental studies of ITG threshold in JET plasmas have confirmed the existence of a critical value of R/L_{Ti}, which is found in close agreement with linear gyro-kinetic calculations. The ion stiffness level is high and keeps R/L_{Ti} close to the linear threshold irrespective of the amount of core ion heating. This finding is not in agreement with non-linear GS2 calculations, yielding significantly higher R/L_{Ti} values than the linear threshold. The stiffness level appears to decrease with increasing toroidal rotation, an effect not evidenced up to now either in experiments or in theoretical predictions. The results call for further theoretical and experimental investigations in view of their impact on the interpretation of present-day experiments and correct extrapolation of present results to ITER/DEMO.

References

[1] A.G.Peeters *et al.*, Nucl. Fusion **42,** 1376 (2002)

[2] C.C.Petty *et al.*, Phys. Plasmas **9**, 128 (2002)

[3] R.C.Wolf *et al.*, Plasma Phys. Controlled Fusion **45,** 1757 (2003)

[4] Mattor N. *et al.*, Phys. Fluids **31**, 1180 (1988)

[5] F.Romanelli et al., Phys. Fluids B **1**, 1018 (1989)

[6] J.W.Connor and H.R.Wilson, Plasma Phys. Controlled Fusion **36,** 719 (1994)

[7] M.Kotschenreuther *et al.*, Phys. Plasmas **2**, 2381 (1995)

[8] G.Tardini *et al.*, Nucl. Fusion **42,** 258 (2002)

[9] P.Mantica and F.Ryter, C. R. Physique **7,** 634 (2006)

[10] D.R.Mikkelsen *et al.*, Nucl. Fusion **43,** 30 (2003)

[11] F.Ryter et al., "Simultaneous analysis of ion and electron heat transport by power modulation in JET " this conference, EX/P5-19

[12] F.Ryter *et al.*, Phys.Rev.Lett. **95**, 085001-1 (2005)

[13] F.Ryter *et al.*, Plasma Phys. Controlled Fusion **48,** B453 (2006)

[14] A.G. Peeters *et al.*, Phys. Plasmas **12**, 022505 (2005)

[15] X.Garbet et al., Plasma Phys. Control. Fusion **46** (2004) B557–B574

[16] A.M. Dimits *et al.*, Phys. Plasmas **7**, 969 (2000)

[17] X.Garbet *et al.*, Plasma Phys. Controlled Fusion*, **46,** 1351 (2004)

[18] J. Hedin *et al.*, Nucl. Fusion **42**, 527 (2002)

[19] C.D. CHALLIS et al., *Nucl. Fusion, **29,** 563 (1989)

[20] L-G ERIKSSON et al., *Nucl. Fusion*, **33,** 1037 (1993)

[21] R. E. WALTZ et al., *Phys. Plasmas*, **4**, 2482 (1997)

[22] G.CENACCHI and A.TARONI, "JETTO: A free boundary plasma transport code (basic version)", Rapporto ENEA RT/TIB 1988 (5)

[23] R.E. Waltz *et al.*, Phys. Plasmas **1**, 2229 (1994)

[24] J. Kinsey *et al.*, Phys. Plasmas **14,** 102306 (2007)

[25] G.V. PEREVERZEV et al., ASTRA: an automatic system for transport analysis in a tokamak, *Max-Planck-IPP Report* IPP 5/98 (2002)

[26] Suttrop W *et al* 2001 *Europhys. Conf. Abstr.* A **25** 989

[27] F.G.Rimini and G.Saibene, Nucl. Fusion 42 (2002) 86–93

[28] P.C. de Vries, et al., Nucl. Fusion 48 (2008) 065006

[29] M. Kotschenreuther et al., Comput. Phys. Commun. **88 (**1995) 128

[30] F. Jenko et al., Plasma Phys. Controlled Fusion **47**, B195 2005

[31] Peeters A.G. *et al.*, Phys. Plasmas **11**, 3748 (2004)

[32] J. Candy and R. E. Waltz, J. Comput. Phys. **186**, 545 (2003)

[33] T.C. Luce, *et al.*, in Fusion Energy 2006 (Proc. 21st Int. Conf. Chengdu, 2006) (Vienna: IAEA) CD-ROM file PD-3

[34] H.Urano et al., Nucl. Fusion **48,** 085007 (2008)

[35] G.Saibene et al., in Proc. 34th European Physical Society Conference on Plasma Physics, Warsaw, 2007, ECA Vol.31F, O-4.001 (2007)

[36] Y.Liang et al., Phys.Rev.Lett, **98,** 265004 (2007)